

EPR Study of Manganese(II) and Copper(II) in Single Crystals of the Spin-Crossover Complex $\text{Fe}(\text{PTZ})_6(\text{BF}_4)_2$

A. Ozarowski and B. R. McGarvey*

Received November 2, 1988

The complex hexakis(1-propyltetrazole)iron(II) bis(tetrafluoroborate) undergoes an abrupt and complete high-spin-low-spin transition, accompanied by a color change, at 128 K. Large single crystals of that complex doped with Mn(II) or Cu(II) were prepared and investigated by the EPR technique over the temperature range 77–295 K. The zero-field-splitting parameters found for Mn(II) in the paramagnetic phase $D = 184.8 \times 10^{-4} \text{ cm}^{-1}$, $E = 0$, $(F - a) = -18.8 \times 10^{-4} \text{ cm}^{-1}$ suggest a symmetry of a trigonally distorted octahedron about the metal ion. The spectrum of only one molecular entity is seen at all orientations. Two crystallographically different phases have been detected below the high-spin-low-spin transition. Diamagnetic phase I is formed when a paramagnetic sample is quickly cooled to a temperature well below the transition temperature. The ZFS parameters for Mn(II) in phase I of $D = 153.7 \times 10^{-4} \text{ cm}^{-1}$, $E = 0$, $(F - a) = -24.2 \times 10^{-4} \text{ cm}^{-1}$ indicate the continued presence of the 3-fold axis at the Mn(II) site. The directions of the ZFS tensor axes also remain unchanged, and only one molecular entity is seen at all orientations. This phase appears to retain the crystal and molecular structure of the parent paramagnetic state. Diamagnetic phase II is generated either by cooling the paramagnetic sample slowly through the spin-transition temperature or by raising the temperature of diamagnetic phase I to around 120 K and holding it at that temperature for a sufficiently long time. Phase II is then stable down to 77 K. In phase II, three differently oriented molecular entities are seen in the EPR spectra. Both the orientation of the ZFS tensor and the magnitude of D ($240 \times 10^{-4} \text{ cm}^{-1}$) are very different from those observed for the paramagnetic phase, indicating a change in the crystal symmetry. The spectra of Mn(II) doped into hexakis(1-propyltetrazole)zinc(II) bis(tetrafluoroborate) show features similar to those found for the paramagnetic phase and diamagnetic phase I of the iron compound. The dynamic Jahn-Teller effect is observed for Cu(II) in the paramagnetic phase, resulting in an EPR isotropic spectrum with $g_{\text{av}} = 2.16$, $A(\text{Cu})_{\text{av}} = 54 \times 10^{-4} \text{ cm}^{-1}$. A spectrum consistent with a completely frozen JT effect was observed for diamagnetic phase II below 120 K with $g_{x,y} = 2.076$, $g_z = 2.303$, $A(\text{Cu})_{x,y} = 0$, $A(\text{Cu})_z = 166 \times 10^{-4} \text{ cm}^{-1}$. The JT effect is partially dynamic in diamagnetic phase I even at 77 K, indicating a higher symmetry for the copper coordination sphere in this diamagnetic phase as compared to diamagnetic phase II. For many spin-crossover compounds in which a crystallographic phase change occurs along with the spin transition, it is never clear whether the spin change is caused by the crystallographic change or the spin change is the result of the crystallographic change. The fact that the spin change can be observed both with and without a crystallographic phase change in the compound studied here indicates that in this case the crystallographic change is caused by the spin transition.

Introduction

The temperature-induced spin-state transitions in iron(II) complex compounds are encountered if the spin-pairing energy is comparable to the crystal field splitting:^{1,2}

$$10Dq = 2.195B + 3.708C \quad (1)$$

where B and C are the Racah parameters of interelectronic repulsion. A considerable number of iron(II) compounds have been synthesized showing the "crossover" phenomena. The transitions may be of either continuous type, i.e. occurring over an extended temperature range, or discontinuous type, occurring over a narrow temperature range, showing hysteresis and often being associated with crystallographic phase transitions. In the macroscopic description, the gain in entropy appears to be a driving force for the transition.^{1,2} On the molecular level, the importance of the Jahn-Teller effects for discontinuous transitions has been emphasized by Kambara.^{3,4}

An abrupt spin-state transition in $\text{Fe}(\text{PTZ})_6(\text{BF}_4)_2$ (PTZ = 1-propyltetrazole) was first discovered by Franke et al.⁵ The HS-LS transition occurred at 128 K, while the LS-HS transition occurred at 134 K. The spin-state change was accompanied by a color change—the paramagnetic phase was white, while the diamagnetic phase was purple. Electronic,^{6,7} Mössbauer,^{8,9} and IR^{5,8,10} spectra as well as magnetic susceptibility studies^{5,6,8} on

both phases have been reported. It has been shown that at temperatures below 50 K the LS-HS transition may be induced by irradiating into the ${}^1A_{1g} \rightarrow {}^1T_{2g}$ absorption band and the system remains trapped in the high spin state but may be pumped back by irradiating into the ${}^5T_{2g} \rightarrow {}^5E_g$ absorption band.^{6,7,9,10} The phenomenon is called "light-induced excited-spin-state trapping", or LIEST. The 1-propyltetrazole ligand also forms hexacoordinated complexes with divalent ions of Co, Ni, Cu, and Zn that are all isomorphous,⁵ and hence the preparation of mixed crystals is possible.

In this paper we report the results of EPR investigations on single crystals of the title compound doped with corresponding manganese(II) and copper(II) complexes. The dopant acts as a probe that is sensitive to changes in its environment which are caused by the crossover transition of host lattice. Such a method has been applied successfully before to study the spin-state transitions in iron(II) compounds.¹¹⁻¹³ We discovered that two different diamagnetic phases may be generated depending on the rate at which a sample is driven through the crossover transition. The structure of the diamagnetic phase generated by quick cooling is similar to the structure of the paramagnetic phase, while the diamagnetic phase formed by slow cooling is substantially different.

Experimental Section

A. Preparation of the Ligand. 1-Propyltetrazole was prepared from propylamine hydrochloride, NaN_3 , and triethyl orthoformate as described in the literature.^{5,14}

B. Preparation of Complexes. The Fe(II), Mn(II), and Cu(II) complexes were prepared by using tetrafluoroborate salts as described by

- (1) Gütlich, P. *Struct. Bonding (Berlin)* **1981**, *44*, 83.
- (2) König, E.; Ritter, G.; Kulshreshtha, S. K. *Chem. Rev.* **1985**, *85*, 219.
- (3) Kambara, T. *J. Chem. Phys.* **1979**, *70*(9), 4199.
- (4) Kambara, T. *J. Chem. Phys.* **1981**, *74*(8), 4557.
- (5) Franke, P. L.; Haasnoot, J. G.; Zuur, A. P. *Inorg. Chim. Acta* **1982**, *59*, 5.
- (6) Decurtins, S.; Gütlich, P.; Hasselbach, K. M.; Hauser, A.; Spiering, H. *Inorg. Chem.* **1985**, *24*, 2174.
- (7) Hauser, A.; Gütlich, P.; Spiering, H. *Inorg. Chem.* **1986**, *25*, 4245.
- (8) Müller, E. W.; Enslin, J.; Spiering, H.; Gütlich, P. *Inorg. Chem.* **1983**, *22*, 2074.
- (9) Decurtins, S.; Gütlich, P.; Köhler, C. P.; Spiering, H. *Chem. Phys. Lett.* **1984**, *105*, 1.

- (10) Baldenius, K. U.; Campen, A. K.; Höhnk, H. D.; Rest, A. J. *J. Mol. Struct.* **1987**, *157*, 295.
- (11) Rao, P. S.; Reuveni, A.; McGarvey, B. R.; Ganguli, P.; Gütlich, P. *Inorg. Chem.* **1981**, *20*, 204.
- (12) Ozarowski, A.; McGarvey, B. R.; Sarkar, A. B.; Drake, J. E. *Inorg. Chem.* **1988**, *27*, 628.
- (13) Vreugdenhil, W.; Haasnoot, J. G.; Kahn, O.; Thury, P.; Reedijk, J. J. *Am. Chem. Soc.* **1987**, *109*, 5272.
- (14) Kamiya, T.; Saito, Y. *Ger. Offen.* P2147023.5, 1971.

Franke et al.⁵ Doped single crystals were grown from aqueous solutions containing 1–2% of the dopant with respect to the iron compound. Crystals as large as 4 × 4 × 1 mm could be obtained. The crystals were colorless and transparent and had a shape of thin hexagonal plates. Their single-crystal nature was confirmed by EPR spectra.

C. EPR Spectra. EPR spectra were recorded on a Varian E12 spectrometer equipped with a rotating cavity and rotating base magnet. The Varian nitrogen-flow cooling system was used to perform the variable-temperature studies, and an insert type Dewar flask was employed to record the spectra at the fixed temperature of 77 K. The linearity and absolute strength of the magnetic field was calibrated by using a home-built variable-frequency proton NMR spectrometer whose frequency was measured by a frequency counter. The single crystals were mounted on quartz rods.

Results

A. Spin Hamiltonian Parameters. The systems that could be well characterized gave a spectrum of one molecular entity whose zero-field splitting was smaller than the microwave quantum energy, and further they displayed cylindrical symmetry; that is, the spectrum remained constant in a plane perpendicular to the direction in which the maximum zero-field splitting (ZFS) was observed. This direction of maximum ZFS is taken to be the *z* axis for the ZFS tensor. The X-ray structure (see below) showed a regular octahedron for the ligands surrounding the iron ion, but the presence of a large zero-field splitting in our spectra indicated a deviation from exact octahedral symmetry. Since the maximal ZFS corresponds to the 3-fold axis of the crystal and the ligand octahedron, we have taken the distortion to be trigonal with a spin Hamiltonian of the following form:^{15–18}

$$\hat{H} = \beta H \cdot g \cdot \hat{S} + D[\hat{S}_z^2 - \frac{1}{3}S(S+1)] + E(\hat{S}_x^2 - \hat{S}_y^2) + \frac{(F-a)}{180}[35\hat{S}_z^4 - 30S(S+1)\hat{S}_z^2 + 25\hat{S}_z^2 - 6S(S+1) + 3S^2(S+1)^2] - \frac{\sqrt{2}}{36}a[\hat{S}_z(\hat{S}_+^3 + \hat{S}_-^3) + (\hat{S}_+^3 + \hat{S}_-^3)\hat{S}_z] + \hat{S} \cdot A \cdot \hat{I} \quad (2)$$

where¹⁸ $(F-a) = 180B_4^0$, $a = 9B_4^3/\sqrt{2}$, and the trigonal axis is the axis of quantization.

The cylindrical symmetry of the spectra implies a zero value for the *E* parameter. The electronic Zeeman and nuclear hyperfine interactions are taken to be isotropic. This is not exactly true but is generally found to be a reasonable approximation for the spherically symmetric ⁶A state of Mn(II). The parameters of the spin Hamiltonian were found by fitting of the spectra measured at both orientations $H \parallel z$ and $H \perp z$. The matrix of the Hamiltonian without the hyperfine term $\hat{S} \cdot A \cdot \hat{I}$ was diagonalized by using the Householder transformation.¹⁹ The hyperfine term $\hat{S} \cdot A \cdot \hat{I}$ was then treated as a perturbation and calculated up to the second order. All 60 allowed lines (total at both orientations) were calculated to within 5 G from their experimental positions. All transition fields and probabilities were calculated over the magnetic field range 0–0.5 T. The second-order corrections in the hyperfine interaction produce a characteristic pattern in the hyperfine splittings that is determined by the signs of the ZFS parameters relative to *A*.^{12,17} Since *A* is always negative, this allowed us to fix the signs of *D* and $(F-a)$. The parameters found in this way were used to calculate the angular dependencies yielding a good agreement with the experiment. In trigonal symmetry only the value of $(F-a)$ can be found from spectra measured at only $H \parallel z$ and $H \perp z$. Spectra measured at intermediate orientations are needed to determine the magnitudes of *F* and *a* separately. Unfortunately, in our case the spectra recorded at orientations

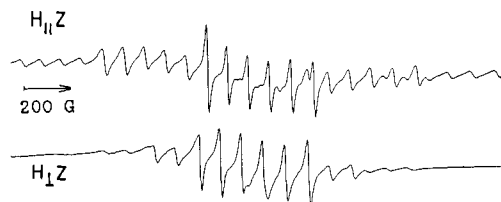


Figure 1. Single-crystal EPR spectra of Mn(II) in Fe(PTZ)₆(BF₄)₂ at room temperature.

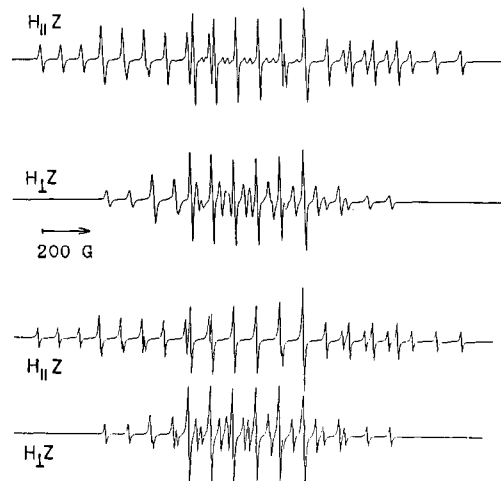


Figure 2. Single-crystal EPR spectra of Mn(II) in the diamagnetic phase I of Fe(PTZ)₆(BF₄)₂ at 77 K. The top spectra are experimental, and the bottom spectra are simulated by using parameters from Table I.

Table I. Spin Hamiltonian Parameters for Mn(II)

	<i>T</i> , K	<i>g</i>	<i>D</i> ^a	<i>E</i> ^a	$(F-a)$ ^a	<i>A</i> ^a
In Fe(PTZ) ₆ (BF ₄) ₂						
paramag phase	290	1.999	184.8	0	-18.8	-85
diamag phase I	77	1.999	153.7	0	-24.2	-85
diamag phase II	77	2	240	<i>b</i>	<i>b</i>	-85
In Zn(PTZ) ₆ (BF ₄) ₂						
	290	1.999	181.2	0	-17.0	-85
	77	1.999	169.9	0	-22.6	-85

^aUnits in 10⁻⁴ cm⁻¹. ^bImpossible to determine due to poor quality of spectra.

far from parallel and perpendicular to the trigonal axis were of poor quality with only the central group being well resolved. The patterns of hyperfine splittings at all orientations were better simulated with *a* = 0 than with *F* = 0. Therefore, it seems that *F* is the dominant term.

For Cu(II) the spin Hamiltonian used was^{15–17}

$$\hat{H} = \beta(g_x H_x S_x + g_y H_y S_y + g_z H_z S_z) + [A(\text{Cu})_x S_x I_x + A(\text{Cu})_y S_y I_y + A(\text{Cu})_z S_z I_z] + [A(\text{N})_x S_x I_x + A(\text{N})_y S_y I_y + A(\text{N})_z S_z I_z] \quad (3)$$

In this case the parameters were determined by fitting the experimental spectra to a second-order perturbation solution of the above Hamiltonian.

B. Mn(II) in Fe(PTZ)₆(BF₄)₂. The EPR spectra of single crystals of Fe(PTZ)₆(BF₄)₂ doped with Mn(II) showed a typical pattern of five groups split into six lines each, indicating a $S = 5/2$, $I = 5/2$ system with the zero-field splitting smaller than the microwave quantum energy at X-band frequency. A spectrum of only one molecular entity was clearly observed at all orientations. Separation between hyperfine lines within each fine pattern was not constant, the last fine group showing the largest hyperfine splitting (Figures 1 and 2). The ZFS was maximal when the magnetic field was perpendicular to the plane of the hexagonally shaped crystals. Thus, the direction defined in this way may be chosen as a *z* axis for the zero-field-splitting tensor. The spectra were quite well resolved at room temperature when *H* was parallel

- (15) McGarvey, B. R. In *Transition Metal Chemistry*; Carlin, R. L., Ed.; Marcel Dekker: New York 1966; Vol. 3, p 169.
 (16) Bencini, A.; Gatteschi, D. In *Transition Metal Chemistry*; Melson, G. A., Figgis, B. N., Eds.; Marcel Dekker: New York, 1982; Vol. 8, p 33.
 (17) Abragam, A.; Bleaney, B. In *Electron Paramagnetic Resonance of Transition Ions*; Clarendon: Oxford, England, 1970.
 (18) Rudowicz, C. *Magn. Reson. Rev.* **1987**, *13*, 1.
 (19) Wilkinson, J. H. In *The Algebraic Eigenvalue Problem*; Clarendon: Oxford, England, 1965; p 290.

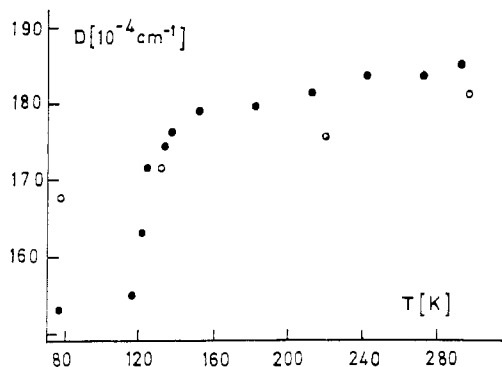


Figure 3. Temperature dependencies of the D parameter for Mn(II): (●) doped into $\text{Fe}(\text{PTZ})_6(\text{BF}_4)_2$; (○) doped into $\text{Zn}(\text{PTZ})_6(\text{BF}_4)_2$.

to z . The line widths (except those in the central pattern) increased considerably, however, as crystals were rotated away from this orientation, and consequently, the amplitude decreased. When the magnetic field was (nearly) perpendicular to the z axis, the spectra were well resolved again. If a crystal was rotated about the z axis, i.e. the magnetic field was in the xy plane, the spectra exhibited no angular dependence at all. In the powder spectra the outermost signals corresponding to the z orientation were not observed, even at a very increased gain, presumably owing to strong angular dependencies of resonance fields on the one hand and to angular dependencies of line widths on the other hand. Powder spectra were thus very similar to the spectra of single crystals recorded in the xy plane. The presence of forbidden doublets between the six lines in the central multiplet show that the crystal was never perfectly aligned with $H \parallel z$. Our simulations showed that a misalignment of only a few degrees was sufficient to give these "forbidden" signals the observed intensity.

The temperature dependence of the EPR spectra was investigated in single crystals with H parallel to z , as the spectra in this orientation had the best resolution. In cooling, the paramagnetic phase was stable down to 130 K. Cooling to 200 K caused the resolution to deteriorate somewhat and the D parameter to decrease slowly. Below this temperature resolution began to improve, and below 140 K the rate of decrease in D changed dramatically (Figure 3).

The behavior of the crystal during the HS–LS transition and below was found to depend on the rate at which the sample was cooled. We have detected the existence of two different diamagnetic phases. A fast cooling from 130 K (or above) to 110 K (or below) caused the spin transition to occur, accompanied by a color change—colorless, transparent crystals became deeply purple. The transition was complete within less than 1 min. The D parameter and the line widths decreased again, but the EPR spectrum was essentially similar to that found in the paramagnetic phase: the direction of z axis did not change, there was still only one molecular entity, and the spectra showed no angular dependence when a crystal was rotated in the xy plane. Further cooling down to 77 K caused only a slight decrease of D and resolution improvement. Forbidden transitions with $\Delta M_S = 2$ appeared at 77 K with amplitudes 2 orders of magnitude smaller than that of the allowed signals. This species was stable at 77 K for indefinite time—at least for 24 h. This diamagnetic phase will hereafter be referred to as diamagnetic phase I.

When the paramagnetic sample was allowed to remain at ca. 120 K for some time, a completely different spectrum developed slowly (Figure 4). A final state was achieved in 20–60 min. The time required for the transition to be complete was not very reproducible. It may be dependent on crystal quality and on temperature fluctuations. It was found that the crystals were also purple, i.e. diamagnetic at this point, but the new EPR spectrum was poorly resolved with very low intensity and the presence of three differently oriented molecular entities could be inferred from angular dependencies. The D parameter was substantially larger than that found in the spectra of either the paramagnetic phase or the diamagnetic phase produced by the rapid cooling described above. The direction of the z axis for the new species was also

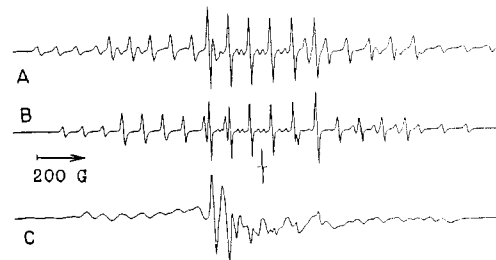


Figure 4. Three types of EPR spectra observed for Mn(II) in $\text{Fe}(\text{PTZ})_6(\text{BF}_4)_2$ at unchanged orientation of a single crystal: (A) paramagnetic phase, 133 K; (B) diamagnetic phase I, 110 K; (C) diamagnetic phase II, 110 K. The DPPH signal at 0.3206 T is also shown.

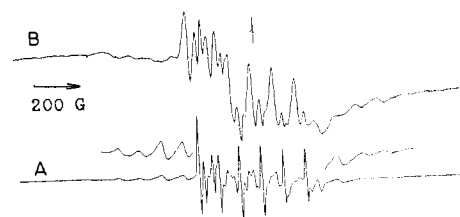


Figure 5. Powder EPR spectra of Mn(II) at 77 K: (A) diamagnetic phase I; (B) diamagnetic phase II. The DPPH signal at 0.3222 T is also shown.

no longer perpendicular to the hexagonal plane of the crystal. Further cooling to 77 K did not cause any substantial changes to this spectrum except a further increase of D . This diamagnetic phase will hereafter be referred to as diamagnetic phase II.

A D value of $240 \times 10^{-4} \text{ cm}^{-1}$ was estimated from the spectrum with the maximal ZFS, recorded with a crystal rotated by 15° from the z axis of the paramagnetic or fast-cooled diamagnetic phases. Because we could rotate crystals in only one plane, it is not certain that we have found an absolute maximum of the ZFS, and hence the D value may be even larger. Very low intensity of the spectra and slow generation of this phase inside the EPR apparatus, as well as the need to use a new crystal for each experiment, were further complications.

The crystals usually appeared to survive a few HS–LS and LS–HS transitions but became more and more turbid after each subsequent experiment and finally cracked. The phenomenon was in this case not as pronounced as in the case of bis(2,2'-bis-2-thiazoline)bis(thiocyanato)iron(II), investigated by us before,¹² where all crystals pulverized at the first LS–HS transition. When a sample was warmed, the spectrum of the paramagnetic phase reappeared at ca. 135 K.

Diamagnetic phase II could also be generated from diamagnetic phase I by warming and maintaining it at 120 K for a few minutes—the transition was relatively fast in this case compared to the transition from the paramagnetic phase. Phase II was stable at 77 K for an indefinite time, at least for 24 h. Phase I could only be produced by rapid cooling from the paramagnetic phase. Both diamagnetic phases could also be generated in powder samples in analogous ways and could be detected through powder EPR spectra (Figure 5).

C. Mn(II) in $\text{Zn}(\text{PTZ})_6(\text{BF}_4)_2$. Single crystals of the zinc complex of the same ligand, doped with Mn(II) have been grown for comparative purposes. The crystals had the same shape as those of the iron complex and were colorless and transparent. The EPR spectra were very similar to those of the iron complex doped with manganese. The D parameter was only slightly smaller for the zinc compound than it was in the iron compound and decreased with decreasing temperature over the range 293–77 K at a rate similar to that found for the iron complex over the range 290–140 K (Figure 3). A spectrum of one molecular entity was seen at all orientations.

D. Cu(II) in $\text{Fe}(\text{PTZ})_6(\text{BF}_4)_2$. Copper-doped $\text{Fe}(\text{PTZ})_6(\text{BF}_4)_2$ were prepared, and the EPR spectra of powder samples at room temperature gave a pattern of four hyperfine lines (Figure 6). A nearly identical spectrum was obtained for a liquid solution of

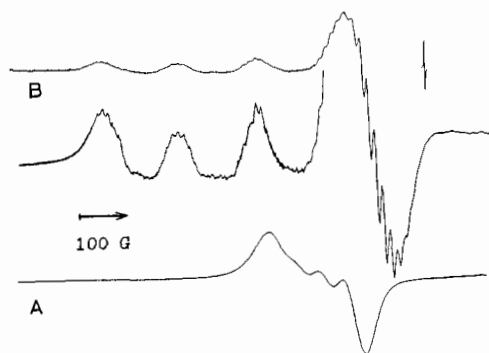


Figure 6. Powder EPR spectra of Cu(II) doped into Fe(PTZ)₆(BF₄)₂: (A) paramagnetic phase, 290 K; (B) diamagnetic phase II, 77 K. The DPPH signal at 0.3228 T is also shown.

Cu(PTZ)₆(BF₄)₂ in methanol. Powder samples of the pure copper complex exhibited similar spectra with somewhat poorer resolution. The single-crystal spectra of the pure copper complex as well as of the copper-doped iron complex showed a similar isotropic spectrum at room temperature.

Cooling to 77 K of the pure copper compound resulted in an anisotropic spectrum with distinct hyperfine structure. The copper-doped iron complex showed an isotropic spectrum in the paramagnetic phase down to the transition temperature. The parameters for this isotropic spectrum were $g_{av} = 2.16$, $A_{av} = 54 \times 10^{-4} \text{ cm}^{-1}$. When the sample was slowly cooled through the transition temperature to produce diamagnetic phase II, a beautifully resolved anisotropic spectrum appeared (Figure 6) with $g_x = g_y = 2.076$, $g_z = 2.303$, $A_x = A_y = 0$, $|A_z| = 166 \times 10^{-4} \text{ cm}^{-1}$. A well-resolved superhyperfine structure due to four nitrogen atoms present in the equatorial plane of the molecule was also seen with $A_N = 14.8 \text{ G}$. The nitrogen coupling constant could not be measured accurately on the parallel portion of the spectrum due to the overlap of ⁶⁵Cu and ⁶³Cu hyperfine lines. It was estimated to be about 12 G.

If a sample (crystal or powder) was passed quickly through the "crossover" to produce diamagnetic phase I, the isotropic component was very pronounced at 110 K and could be seen even at 77 K together with a poorly resolved anisotropic component. The anisotropic component had parameters similar to those found in diamagnetic phase II. No ¹⁴N hyperfine splittings could be observed due to the poorer resolution of the spectra. When this fast-cooled sample was warmed to 120 K, the anisotropic copper spectrum appeared, and further warming to 135 K resulted in the reappearance of the purely isotropic spectrum, characteristic of the paramagnetic phase. Hence, two different diamagnetic phases could also be detected by using copper(II) as a probe.

When copper was doped into the zinc-propyltetrazole complex, an anisotropic EPR spectrum was observed at 77 K with spin Hamiltonian parameters similar to those found in diamagnetic phase II.

EPR parameters can be used to calculate coefficients in the molecular orbitals.^{15-17,20-23} We applied the equations derived by Gersmann and Swalen,²⁰ on the basis of a theoretical treatment of Maki and McGarvey.²¹ The values $T(n) = 0.33$, $P = 0.036 \text{ cm}^{-1}$ were assumed after Maki and McGarvey, but a value of about 0.18 for the group overlap integral was deduced from the data published by Smith,²² which is much larger than that used earlier.^{20,21} The molecular orbital coefficients are only weakly sensitive to the choice of S , however. A negative sign for $A(\text{Cu})_z$ had to be assumed in these calculations. Crystal field splitting energy is $15\,700 \text{ cm}^{-1}$ according to Franke et al.⁵ and thus $\lambda/\Delta = -0.053$. The constant κ was treated as an adjustable parameter. It has been suggested that κ should not be multiplied by α^2 in the equations for copper hyperfine coupling constants.²³ An appro-

prate change in Gersmann's formulae did not cause any changes in the derived values of the MO coefficients in our case, however. The following values were computed: $\alpha = 0.96$ (σ bond), $\beta = 0.96$ (in-plane π bond), $\delta = 0.96$ (out-of-plane π bond), and $\kappa = 0.35$ ($\kappa\alpha^2 = 0.32$). Propyltetrazole would then appear as a ligand weakly covalent toward copper(II).

Some crystals doped with both copper and manganese have been prepared. Analysis of the EPR spectrum from diamagnetic phase II revealed that there are at least two molecular copper entities whose z axes (defined by the direction of g_z) are inclined by some 54° with respect to the z axis of manganese, as defined above, and are perpendicular to each other.

Discussion

The idea of investigating the symmetry of an iron compound by observing EPR spectra of manganese is based on the expectation that a molecule of a manganese complex doped into a host lattice will assume the symmetry of host molecules, since geometry of environment does not affect the energy of the ground state of manganese(II) ions. On the other hand, the zero-field-splitting parameters for a high-spin d^5 ion are indeed very sensitive to the environmental symmetry. We have earlier found¹² that the complex bis(bithiazoline)bis(thiocyanato)iron(II) forms two modifications of which only one exhibits "crossover" (polymorph A), while polymorph B is paramagnetic, although there are only minor differences in molecular structures of A and B. The EPR spectra of manganese doped into both modifications showed similar D parameters but differed in E values, resulting in E/D ratios of 0.27 and 0.09 for polymorphs A and B, respectively. Recently,²⁴ it was shown that molecule B possesses a 2-fold axis, while there are no symmetry elements in the A molecule, and this explains the considerable difference in E values for both species. Values of the spin Hamiltonian parameters D , E , and $(F - a)$ obtained for Mn(II) in Fe(PTZ)₆(BF₄)₂ in this work would indicate a trigonal distortion of the octahedral ligand arrangement around iron ions, although it is not possible to predict its magnitude. The vanishing value of E provides a good test for the presence of only a trigonal distortion. A slightly smaller symmetry deviation of the same kind in the zinc compound may be inferred from the EPR parameters for Mn(II).

The crystal structure of the title compound has been determined at 140 K, i.e. for the paramagnetic phase, by Franke.²⁵ The choice of experimental conditions was somewhat unfortunate, since there was already a small fraction of LS phase at that temperature and this resulted in a high R value. Nevertheless, the data seem to be good enough for our purposes. The compound crystallizes in the rhombohedral space group $R\bar{3}$ with $a = b = 10.865 \text{ \AA}$, $\alpha = \beta = 90^\circ$, $\gamma = 120^\circ$, $Z = 3$. The iron atoms occupy special positions located on the 3-fold axis. Because the z axis of the zero-field-splitting tensor is parallel to the 3-fold axis and EPR spectra show no angular dependence in the xy plane, a spectrum of only one molecular entity is indeed expected at all orientations if a is not large.¹⁷ The crystal packing is rather loose (density of about 1.2 g/cm^3)—the shortest distance between iron atoms is 10.865 \AA . Six monodentate propyltetrazole ligands coordinating via their N(4) atoms appear to form regular octahedra around iron ions. The iron, manganese, and copper compounds are isomorphous.

Long distances between metal atoms obviously reduce magnetic metal-metal-exchange interactions, allowing for the appearance of hyperfine splitting in the spectra of the pure copper complex. The fact that the line widths in the spectra of manganese doped into the iron complex do not increase considerably when the temperature of the paramagnetic phase is lowered may also be attributed to a weak dipole-dipole line-broadening mechanism, resulting from long metal-metal distances.

Two striking changes are observed in the Mn(II) spectra in the temperature region 140–125 K, where the transition becomes discontinuous. One, there is a sudden reduction of line widths

(20) Gersmann, H. R.; Swalen, J. D. *J. Chem. Phys.* **1962**, *36*, 3221.

(21) Maki, A. H.; McGarvey, B. R. *J. Chem. Phys.* **1958**, *29*, 35.

(22) Smith, D. W. *J. Chem. Soc. A* **1970**, 3108.

(23) Rockenbauer, A. *J. Magn. Reson.* **1979**, *35*, 429.

(24) Ozarowski, A.; McGarvey, B. R.; Sarkar, A. B.; Drake, J. E. *Inorg. Chem.* **1988**, *27*, 2560.

(25) Franke, P. L. Thesis, Rijks University, Leiden, 1982.

below 140 K and two, the decrease in the magnitude of D with decreasing temperature becomes much more rapid. The onset of these phenomena parallels the onset of a continuous HS–LS transition (Figure 3). Only a small fraction of iron atoms change their spin state in this interval, however, since most atoms change their spin state below 128 K, where the transition becomes discontinuous. The rapid reduction in the magnitude of D suggests a rapid reduction of the trigonal distortion in the host molecules over the temperature range 140–125 K. The reduction of line width could be associated with the reduction in D .

The quickly cooled diamagnetic phase I has obviously the same symmetry as the paramagnetic phase does, with even a smaller trigonal distortion. This distortion is most likely not caused by the Jahn–Teller effect in Fe(II) (JT effect in the T state may lead to trigonal distortion), since its magnitude is nearly the same in both iron and zinc complexes. The presence of the dynamic Jahn–Teller effect for Cu(II) over the entire temperature range where the paramagnetic phase is stable and to some extent, also, for diamagnetic phase I is a typical phenomenon when Cu(II) ions occupy trigonally distorted pseudooctahedral sites.¹⁷ To our knowledge, this diamagnetic phase I has not been detected before.

The following information about the slowly cooled diamagnetic phase II is presently available: Franke²⁵ found that "at 100 K the crystal was no longer a single crystal in the crystallographic sense", although before the transition it had been. Gütllich et al.²⁶ discovered that the spin transition causes a change of the crystal system: crystals become monoclinic, unit cell volume doubles, and owing to the loss of the 3-fold axis, each crystal splits into three differently oriented domains. No further details are available at this moment. It is apparent that our EPR results are in agreement with the above data. Although no exact values of the spin Hamiltonian parameters could be found in this case, owing to experimental difficulties, the D value is larger by at least 60% than it is in diamagnetic phase I. Hence, a considerable descent in the local molecular symmetry in this phase with respect to both the paramagnetic and diamagnetic phase I is obvious.

Forbidden transitions with $\Delta M_I = 1$ appear in the central pattern ($M_S = 1/2 \leftrightarrow M_S = -1/2$) of the spectra of Mn(II) in the diamagnetic phase II (Figure 5) with an intensity considerably enhanced with respect to the intensity of corresponding signals in the other two phases, most likely as a result of the symmetry lowering. Similar conclusions concerning local symmetry may be inferred from the spectra of Cu(II) for which the dynamic Jahn–Teller effect disappears in diamagnetic phase II indicating, also, a symmetry lowering. When the dynamic Jahn–Teller effect freezes, the main axes for the g tensor are expected to lie along the 4-fold axes of the approximate octahedron¹⁷ formed by six nitrogen atoms; i.e., they should point toward these nitrogen atoms. Up to three directions (perpendicular to each other) for g_z may then be observed. This is in agreement with the angular relations

between the copper and manganese spectra observed for the crystals doped with both copper and manganese: the 3-fold (111) axis of the (approximate) octahedron indeed should form angles of some 54° with the tetragonal axes (see Results, section D).

The EPR parameters found for Mn^{2+} in both $Fe(PTZ)_6(BF_4)_2$ (paramagnetic phase and diamagnetic phase I) and $Zn(PTZ)_6(BF_4)_2$ lead to the conclusion that the molecular symmetry of a trigonally distorted octahedron and the $R\bar{3}$ crystal symmetry are probably "natural" for propyltetrazole complexes with divalent metal ions. Analogous 1-methyltetrazole complexes have been shown to crystallize in the $P2_1/n$ group with two Cu sites of different local symmetries.²⁷ The formation of species of lower symmetry (diamagnetic phase II) must be caused by processes peculiar to the spin transition, involving some rearrangement of the molecules. Our results indicate that the crystallographic phase transformation is rapid near the magnetic transition temperature if the molecules are already in the low-spin state but is slow if both the spin state and crystal structure must change at the same time. We have no explanation of this interesting but unusual observation. The interesting question as to whether or not the bonds in these diamagnetic phases are shorter than those in the paramagnetic molecules cannot be answered definitively on the basis of our EPR results only.

Conclusions

Although there is no X-ray data on diamagnetic phase I, the EPR results tell us it is very similar in structure to the paramagnetic phase in that only one magnetic species is detected at all orientations and the site symmetry of the molecule has a rotational symmetry axis higher than 2-fold. It appears reasonable to assume, therefore, that there is no crystalline phase transformation when the system changes from high spin to low spin (diamagnetic phase I). We have, therefore, in $Fe(PTZ)_6(BF_4)_2$ observed for the first time the same HS–LS transition occurring both with a crystalline phase transformation and without the phase transformation. The further fact that phase I spontaneously goes to phase II at temperatures just below the spin-crossover temperature demonstrates that the crystalline phase transformation is driven by the spin-crossover transition rather than being the cause of the spin-crossover transition. We expect that this is probably true of most systems in which both a spin crossover plus a crystalline phase transition are observed together, but this is the first case where it has been demonstrated so dramatically.

Acknowledgment. This work was supported by an operating grant from the Natural Sciences and Engineering Research Council of Canada. We wish to thank Prof. J. G. Haasnoot of Leiden University for sending us a copy of Dr. Franke's thesis and Prof. P. Gütllich of Mainz University for information on the X-ray studies of $Fe(PTZ)_6(BF_4)_2$.

(26) Gütllich, P. Private communication.

(27) Wijnands, P. E. M.; Maaskant, W. J. A.; Reedijk, J. *Chem. Phys. Lett.* **1986**, *130*(6), 536.